

A community detection analysis of malocclusion classes from orthodontics and upper airway data

Gabriele Di Carlo¹  | Tommaso Gili^{2,3}  | Guido Caldarelli^{3,4}  |
Antonella Polimeni¹  | Paolo M. Cattaneo⁵ 

¹Department of Oral and Maxillo-Facial Sciences, Sapienza University of Rome, Rome, Italy

²Networks Unit, IMT School for Advanced Studies Lucca, Lucca, Italy

³Department of Molecular Sciences and Nanosystems, Ca' Foscari University of Venice, Venezia Mestre, Italy

⁴CNR-ISC Unità Sapienza, Rome, Italy

⁵Melbourne Dental School, Faculty of Medicine, Dentistry and Health Sciences, University of Melbourne, Melbourne, Vic., Australia

Correspondence

Paolo M. Cattaneo, Melbourne Dental School, Faculty of Medicine, Dentistry and Health Sciences, University of Melbourne, 720 Swanston St, Carlton VIC, Melbourne, Vic. 3053, Australia.
Email: paolo.cattaneo@unimelb.edu.au

Abstract

Objective: The interaction between skeletal class and upper airway has been extensively studied. Nevertheless, this relationship has not been clearly elucidated, with the heterogeneity of results suggesting the existence of different patterns for patients' classification, which has been elusive so far, probably due to oversimplified approaches. Hence, a network analysis was applied to test whether different patterns in patients' grouping exist.

Settings and sample population: Ninety young adult patients with no obvious signs of respiratory diseases and no previous adeno-tonsillectomy procedures, with thirty patients characterized as Class I ($0 < ANB < 4$); 30 Class II ($ANB > 4$); and 30 as Class III ($ANB < 0$).

Materials and methods: A community detection approach was applied on a graph obtained from a previously analysed sample: thirty-two measurements (nineteen cephalometric and thirteen upper airways data) were considered.

Results: An airway-orthodontic complex network has been obtained by cross-correlating patients. Before entering the correlation, data were controlled for age and gender using linear regression and standardized. By including or not the upper airway measurements as independent variables, two different community structures were obtained. Each contained five modules, though with different patients' assignments.

Conclusion: The community detection algorithm found the existence of more than the three classical skeletal classifications. These results support the development of alternative tools to classify subjects according to their craniofacial morphology. This approach could offer a powerful tool for implementing novel strategies for clinical and research in orthodontics.

KEYWORDS

malocclusions, network analysis, orthodontics, upper airway

Di Carlo Gabriele and Gili Tommaso contributed equally to the work

Paolo M. Cattaneo: Formerly: Section of Orthodontics, Department of Dentistry and Oral Health, Aarhus University, Aarhus, Denmark.

© 2021 John Wiley & Sons A/S. Published by John Wiley & Sons Ltd

1 | INTRODUCTION

With the introduction of cone beam computed tomography (CBCT), many studies focusing on upper airway morphology have been generated, especially within the orthodontic literature.^{1,2} Back in 2012, Van Vlijmen, based on the then-available evidence, could claim that only the studies assessing airway diagnostics showed a scientific impact of CBCT in the orthodontic field.³ Different aspects were analysed by other authors: effects produced by conventional fixed appliance therapy and/or orthognathic surgery, effects produced by extractive treatments and outcomes generated by functional appliance therapy.⁴⁻¹⁰ Among them, a special interest was devoted to the possible relationships between airway dimensions and different anteroposterior facial patterns.¹¹⁻¹⁸ The interest in elucidating these relationships is not new: airway and the naso-respiratory function have been in the centre of interest among orthodontists since the seventies.^{19,20} Despite the large number of studies produced, in 1990 Warren and Spalding stated that the relationship between naso-respiratory function and dentofacial development is anyhow controversial. They postulated that the lack of evidence was most probably related to the shortcomings of two-dimensional (2D) cephalometric measurements as the sole indicators for the upper airways' dimensions.²¹ Indeed, the controversial results about the relationships between craniofacial anatomy and airway dimension and morphology could be ascribed to the methods applied and the parameters chosen for assessing the upper airway. The 3D information provided by CBCT has the potential to overcome this obstacle. Nevertheless, the controversy became even more complex. Some authors claimed the relationship between skeletal anteroposterior facial patterns and airway volumes,^{12-14,17,22} while many others could not reach the same conclusions.^{16,18,23-25}

Although some controversies could be attributed to the lack of consistency between the different methodologies applied, it is believed that assessing the three-dimensional structure of the skull through the lens of traditional schemes could lead to an underrepresentation of this composite musculo-skeletal craniofacial complex. In fact, this system shows an evident complexity that emerges and evolves during the growing processes, following an intricate cross-action of auxologic forces, distortive processes and compensatory mechanisms. For this reason, network analysis methods started to be considered a good approach to investigate standard orthodontic data.²⁶ In daily clinical activity, the orthodontist must identify and locate the critical points of malocclusion to establish objectives, strategies, priorities and treatment sequences. For this reason, it is common practice to divide the morphometric features into three main classes: Class I, Class II and Class III. On the contrary, the heterogeneity of results regarding the link between airway and craniofacial morphology suggests the existence of a different pattern of patient grouping, which has been elusive so far. A possible approach for describing craniofacial complexity can be to look at it as a network and distinguish and visualize the most interconnected clinical data, radiographic representations and functional mechanisms.²⁷ Moreover, Barabasi suggested studying the interactions of

a complex system considering its mutual empowerment, stating that 'the richness of interactions makes that the whole system is greater than the sum of its parts, due to cooperation phenomena between structures, connectivity'.²⁸ A network analysis allows studying a relevant number of interconnected factors simultaneously by visualizing them in a simplified representation, capturing the structures of co-occurrence between them.²⁹ As we stated in a paper belonging to the same special issue, a complex system of interacting agents takes a natural mathematical form of a graph where the vertices are the system elements, and their complex interaction is put in the form of an edge.^{28,29} By taking into account patients' variability, network theory can optimize the correct diagnosis in precision medicine modelling. Therefore, by applying the complex network methods to the field of orthodontics, it can enable the identification of some general rules governing the growth and development of the entire craniofacial system, which has been vague so far.^{27,30}

1.1 | Aim

To verify the existence of different patient grouping patterns, besides the traditional skeletal and dental malocclusion classification, and assess their correlation with upper airway measurements. A network analysis of the cephalometric measurements will be performed, including and excluding areas and volumes of the upper airways. A community detection approach will be applied to test the null hypothesis that similar clusters of subjects exist within the network.

2 | MATERIALS AND METHODS

2.1 | Subjects

Pre-treatment CBCT scans of 90 young adults, consisting of 32 males and 58 females (13-43 years of age), were obtained from the available records from the clinic of the Section of Orthodontics, Aarhus University. All data used in this study have been previously analysed and published.²³ Only the fully anonymized results from the descriptive tables (Tables 1-4) were used in the present article, making it unnecessary for an Ethical Committee's approval.

The patients included in this study represent the three different skeletal patterns: 30 subjects were Class I ($0 < ANB < 4$); 30 Class II ($ANB > 4$); and 30 Class III ($ANB < 0$). The characteristics of the entire sample are described in Table 3, while the characteristics of the sample divided according to the three classes are reported in Table 4. The inclusion criteria were the existence of a 12" CBCT scan (NewTom 3G; QR srl.) taken in occlusion and with patients in a supine position. The CBCT scanner used to scan the patients is provided with a bed, where the patient is lying, with his head fitted in a moulded pillow, making the patient positioning procedure highly reproducible. The exclusion criteria were patients with previous orthodontic treatment, orthognathic surgery, syndromes, pathology involving the upper airway, previous adeno-tonsillectomy procedure

**TABLE 1** List and definition of the cephalometric landmarks used in the upper airway analysis

	Measurements	Description
Skeletal	A	Position of the deepest concavity on anterior profile of the maxilla
	ANS	Tip of anterior nasal spine
	B	Most posterior point on the anterior contour of the lower alveolar process
	Ba	Most postero-inferior point on the clivus
	GH-l	Greater horn of the hyoid bone left
	GH-r	Greater horn of the hyoid bone right
	GoL	The most inferior-posterior point on the left angle of the mandible
	GoR	The most inferior-posterior point on the right angle of the mandible
	H	Uppermost point of the hyoid bone
	ii	A point midway between the incisal edges of the maxillary and mandibular central incisors
	Me	The most inferior point of the bony symphysis anteriorly
	MoL	The distal tip of the first left molar in the jaw of interest
	MoR	The distal tip of the first right molar in the jaw of interest
	N	The intersection of the internasal and frontonasal sutures in the midsagittal plane
	OrR	The most inferior anterior point on right orbit's margin
	OrL	The most inferior anterior point on left orbit's margin
	PNS	The most posterior point on the bony hard palate
	PI	Centroid of the greater palatine foramen left
	Pr	Centroid of the greater palatine foramen right
	PoL	Most superior point of the outline of the external auditory meatus left
	PoR	Most superior point of the outline of the external auditory meatus right
	PoG	The most anterior point of the bony chin in the midsagittal plane
	S	Midpoint of the sella turcica
	So	Midpoint of the sella-basion line
	Zs-L	The most inferior point of the left zygomaticomaxillary suture
	Zs-R	The most inferior point of the right zygomaticomaxillary suture
Airway	ad1	Intersection of the line PNS-Ba and the posterior nasopharyngeal wall
	ad2	Intersection of the line PNS-So and the posterior nasopharyngeal wall
	P3	Intersection between the posterior pharyngeal wall and the bisected Occlusal plane (OP)
	T2	Intersection between the contour of the tongue and the bisected OP
	E	Most superior point of epiglottis
	E1	Frontal wall of pharyngeal airway over E1-E2 line
	E2	Posterior wall of pharyngeal airway over E1-E2 line

and subjectively perceived respiratory problems, as retrieved from the patients' records.

2.2 | 3D image processing and determination of landmarks

All CBCT scans were reconstructed with an isotropic voxel dimension of 0.36 mm. The original data sets were checked and, if needed, re-oriented using as references the upper orbits, Frankfurt plane, the 'Dens' of the second cervical vertebrae and the anterior nasal spine. The CBCT data were then exported via the DICOM format and imported into a specific software program

(Mimics 15.0 Materialise). The data used in the present article were generated and reported as described previously by Di Carlo and coauthors (Tables 1-4; Figure 1).²³ In particular, the following data were considered in the present study: nineteen cephalometric linear measurements, four upper airway volumes (three partial volumes and the total volume) and nine upper airway data. (Tables 1 and 2 and Figure 1).

2.3 | Data pre-processing

According to their diagnostic classes, the targeted orthodontic profiling was performed for three distinct groups, each consisting of 30

TABLE 2 Definition of the linear and angular measurements performed on facial skeleton and upper airway measurements

Skeletal measurements			
Sagittal	S-N-Pog	(deg)	Angle formed by Sella, Nasion and Pogonion
	SNA	(deg)	Angle measuring the anteroposterior relationship of the maxillary basal arch on the anterior cranial base
	SNB	(deg)	Angle measuring the anteroposterior relationship of the mandibular basal arch in relation to the anterior cranial base
	ANB	(deg)	Angle showing the anteroposterior relationship between the maxillary and mandibular apical bases
	S-Pog	(mm)	Distance from Sella point to Pogonion
	PNS-Ba	(mm)	Sagittal depth of the bony nasopharynx
	Ba-Me	(mm)	Distance between Ba point and Me point
	A-Frank perp	(mm)	Distance from A point to Frankfurt Perpendicular passing through Sella point
	B-Frank perp	(mm)	Distance from B to Frankfurt Perpendicular passing through Sella point
	Pog-Frank perp	(mm)	Distance from Pog to Frankfurt Perpendicular passing through Sella point
Vertical	H to palatal	(mm)	Distance between H point to palatal plane
	ANS-Me	(mm)	Distance between Anterior Nasal Spine and Menton
	N-Pog	(mm)	Distance between N point to Pogonion
	PFH	(mm)	Posterior Facial Height, Distance between Sella point and plane comprising: Gor, Gol, B point
Transversal	Gonial width	(mm)	Distance between Gonion right and Gonion left
	Palatal width	(mm)	Distance between Palatal right and Palatal left
	Hyoid width	(mm)	Distance between Greater Horn Right and left
	Zygomatic width	(mm)	Distance between Zs-R to Zs-L
Others	S-N-Ba	(deg)	Angle comprise Nasion Sella and Basion
Airway measurements			
Linear	Ad1-PNS transversal	(mm)	The most transversal extension of the Upper Airway measured at Ad1-PNS level
	Ad1-PNS sagittal	(mm)	The most sagittal extension of the Upper Airway measured at Ad1-PNS level
	T2-P3 transversal	(mm)	The most transversal extension of the Upper Airway measured at T2-P3 level
	T2-P3 sagittal	(mm)	The most sagittal extension of the Upper Airway measured at T2-P3 level
	E1-E2 transversal	(mm)	The most transversal extension of the Upper Airway measured at E1-E2 level
	E1-E2 sagittal	(mm)	The most sagittal extension of the Upper Airway measured at E1-E2 level
Area	Ad1-PNS surface	(mm ²)	The cross-sectional surface measured at Ad1-PNS level
	T2-P3 surface	(mm ²)	The cross-sectional surface measured at T2-P3 level
	E1-E2 surface	(mm ²)	The cross-sectional surface measured at E1-E2 level

subjects. In order to use a homogeneous approach, a unique data set was created, including all of them. Thereby, for each orthodontic metric, patients of the three skeletal classes (I, II and III) were concatenated into a single array, that is $[I_i, II_i, III_i]$ (with $i = 1, \dots, 30$).

Consequently, the data were transformed into Z scores across subjects: for each orthodontic measure 's' and each subject 'k', the Z score $Z_s(k)$ was calculated as Equation (1)

$$Z_s(k) = \frac{s_k - \sum_{k=1}^N s_k}{\frac{1}{N} \sqrt{\sum_{k=1}^N (s_k - \frac{1}{N} \sum_{k=1}^N s_k)^2}} \quad (1)$$

N denoted the total number of subjects. A regression procedure was implemented to reduce the variance across patients of each

orthodontic measure.³¹ The independent variables of the regression (transformed into Z scores) included age, gender and nine uncorrelated upper airway measures (Ad1-PNS surface, T2-P3 surface, E2-E1 surface, Ad1-PNS transversal, T2-P3 transversal, E2-E1 transversal, Ad1-PNS sagittal, T2-P3 sagittal and E2-E1 sagittal) (Table 4).

2.4 | Network analysis

The residuals of the regression were entered in Pearson's cross-correlation analysis, which returned a symmetric correlation matrix. This matrix (the weighted adjacency matrix) can be associated with the undirected and weighted graph of subjects where the weight of a link between two nodes (ie, two patients) is the covariance across



TABLE 3 Descriptive statistics of the linear and angular measurements performed on the facial skeleton and of the measurements performed on upper airways for the entire sample

	Level	Mean	SD	Minimum	Maximum
Skeletal					
Angular (deg)	ANB	2.4	4.2	-8.8	11.5
	SNA	81.3	4.0	71.5	93.0
	SNB	78.6	4.6	67.9	97.8
	S-N-Ba	128.8	4.9	117.8	141.2
	S-N-Pog	79.8	4.6	69.4	97.4
Sagittal (mm)	S-Pog	120.6	7.8	100.7	140.2
	PNS-Ba	42.3	4.2	31.3	55.6
	Ba-Me	105.2	7.5	89.2	132.4
	A-Frank perp	91.1	5.3	79.2	102.9
	B-Frank perp	87.4	7.2	72.6	106.5
Vertical (mm)	Pog-Frank perp	89.1	8.3	68.2	109.3
	H to palatal	59.8	7.9	42.3	85.3
	ANS-Me	67.4	6.8	48.1	85.4
Transversal (mm)	N-Pog	112.0	8.3	86.4	132.5
	PFH	75.4	6.8	59.8	92.9
	Gonial width	87.5	6.4	71.7	101.1
	Palatal width	30.0	2.8	24.1	36.7
	Hyoid width	39.7	4.8	30.5	54.0
	Zygomatic width	82.3	5.8	61.6	96.6
Airway					
Linear (mm)	ad1-PNS	21.3	4.6	6.8	30.3
	T2-P3	17.2	4.0	6.3	28.3
	E1-E2	10.8	2.5	5.0	17.6
Transversal (mm)	ad1-PNS	27.1	4.6	15.8	37.8
	T2-P3	22.0	5.2	10.1	41.2
	E1-E1	31.5	5.1	19.4	45.3
Area (mm ²)	ad1-PNS	386.6	113.6	140.4	649.6
	T2-P3	151.0	62.4	50.1	388.3
	E1-E1	274.8	100.7	28.2	655.1
Volume (mm ³)	TV	12647	3557	6914	22178
	LNP	2378	1128	289	5764
	VLP	4358	1555	1093	9626
	ORP	2856	1295	786	8568

orthodontic measures of the two nodes.^{27,29} The weighted adjacency matrix was thresholded by maintaining the graph connected, that is implying that the graph components' number was equal to the graph size.³² Once the final network was obtained, we ran a community detection algorithm to find a possible functional assignment of the subjects to different orthodontic covariance modules. The community detection method (Louvain algorithm) is an optimization of a topological quantity called 'modularity'. The modularity measures the relative density of edges within communities compared to the density of edges connecting those communities. The larger is

the number of edges inside a community, the better the division in communities has been done. Louvain method first explores the possible community division at a local scale, and small communities are then grouped to find the better possible partition.²⁶ We assessed the effect of the upper airway measures regression on the modules' structure by comparing it with the network's modularity obtained by including the sole age and gender as regressors. The dissimilarity of the modular structures obtained using the two approaches has been tested by calculating the Normalized Mutual Information (NMI).³³ NMI ranges from 0 to 1, where 0 signifies that the partitions

			Mean	SD	Minimum	Maximum
Class I (male = 21; female = 9)	Age	(yrs)	19.7	5.6	13.0	32.0
	ANB	(deg)	2.8	0.8	1.2	4.0
	TV	(mm ³)	12670	3539	7290	22178
	LNP	(mm ³)	2585	1079	290	4855
	VLP	(mm ³)	4554	1528	1945	9091
	ORP	(mm ³)	2724	1474	786	8568
Class II (male = 8; female = 22)	Age	(yrs)	22.6	7.7	15.0	43.0
	ANB	(deg)	6.9	1.9	4.4	11.5
	TV	(mm ³)	12272	2588	6914	17337
	LNP	(mm ³)	2581	1143	683	5764
	VLP	(mm ³)	3881	1319	1093	7094
	ORP	(mm ³)	2703	706	1062	4279
Class III (male = 15; female = 15)	Age	(yrs)	21	5	13	31
	ANB	(deg)	-2.5	1.9	-8.8	-0.1
	TV	(mm ³)	12843	4219	7090	22065
	LNP	(mm ³)	2015	1048	289	5063
	VLP	(mm ³)	4598	1664	1859	9626
	ORP	(mm ³)	3119	1505	906	7768

TABLE 4 Descriptive statistics of age, ANB angle and upper airways volumes according to each skeletal class

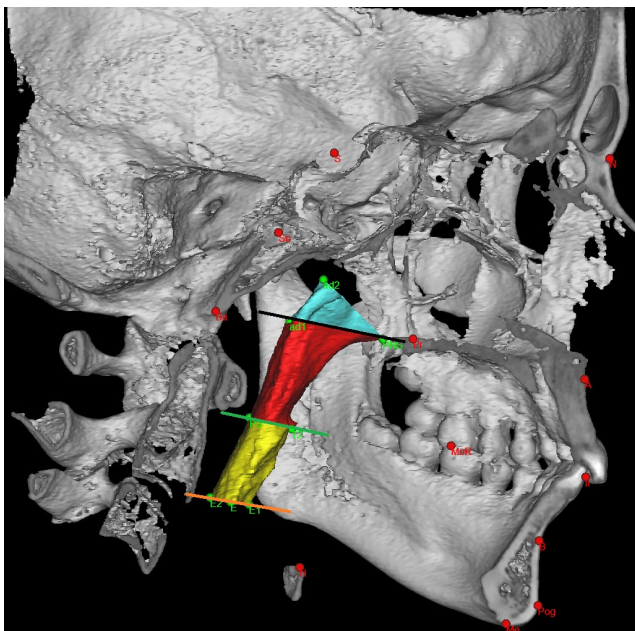


FIGURE 1 Total airway and three partial volumes delimited by eight anteroposterior landmarks. In light blue, the lower nasopharynx (LNP); in red, the velopharynx (VLP); and in yellow, the oropharynx (ORP). The black line identifies the section Ad1-PNS, the green line identifies the section T2-P3, and the orange line identifies the E2-E1 section of the upper airway

are independent and one that they are identical. A permutation procedure assessed the statistical significance of the dissimilarity between the two community structures, which compared the group

similarity in the actual data with permutations (here 10.000) where the group memberships were randomized.³⁴

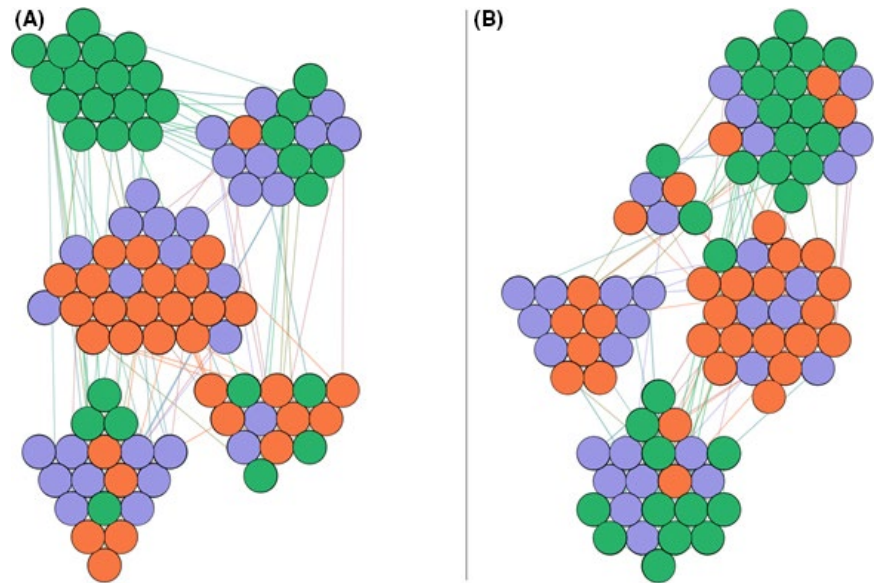
3 | RESULTS

The community detection algorithm returned the nodes' unique assignment to specific subsets according to their connectivity properties. Figure 2 shows the exact structure of the networks obtained by data pre-processed in two different ways, with nodes representing subjects and links representing the existence of significant covariance between two nodes. Different colours of nodes identify different classes, while different groups identify different communities. Specifically, we report two community structures associated with the networks obtained by including or excluding the upper airway measurements as independent variables in the regression part of the pre-processing. In both cases, the number of modules found by the algorithm was five. However, the assignment of patients to each module is different. When airway measurements are included in the regression part of the pre-processing, it can be noticed that Class III patients are more clustered in an independent module (Figure 2A).

In contrast, they are more distributed across modules, particularly in two (Figure 2B). Class I and Class II patients tend to form a big cluster together in both cases, while some heterogeneity characterizes the remaining modules. The NMI calculated for the two community structures was equal to 0.21. The permutation test, which was run over 10 000 permutations, allows the rejection of the null hypothesis (similar structures), with $P < .05$.



FIGURE 2 Community structure of the orthodontic covariance networks. (A) The network was obtained from subject-to-subject correlation after the regression of age, gender and nine upper airways measurements; (B) the network was obtained after the regression of age and gender. The colour code is the same for the two panels: purple = Class I, orange = Class II and green = Class III



4 | DISCUSSION

The present research aimed to verify the existence of different patterns in patients' grouping according to the traditional skeletal and dental malocclusion classification with the upper airway information using a network analysis approach. By applying this approach to a sample comprising 30 subjects in each of the three skeletal patterns (eg, classes I, II and III), the community detection analysis returned five different modules, thus, more than the three traditional classes. The quantitative difference emerging from the present research should be paired to the qualitative differences found in a study using a similar approach proposed by Auconi et al²⁷ In that research, it was found that few highly connected orthodontic features characterized Class II. Simultaneously, Class III patients gave place to a more compact structure due to the co-occurrence of normal and abnormal clinical, functional and radiological features.²⁷ In the present paper, we identified critical peculiarities of malocclusions by restricting our analysis to the strongest correlations. Class I and Class II tend to behave similarly in the two different networks (ie, networks obtained by including or excluding the upper airway measurements as independent variables).

On the other hand, Class III patients tend to form a separate cluster, as previously reported. This tendency is more evident when upper airway measurements are considered. This network analysis suggests that the approach to correlate anteroposterior skeletal patterns could be insufficient to describe the craniofacial system's complexity, which is even more evident when this is correlated with the upper airway. The present study suggests that the controversies in the results obtained trying to link anteroposterior skeletal patterns to airway previously reported in the available literature^{12-14,17,18,22,24} are not exclusively related to methodological drawbacks (eg, segmentation method or acquisition position of the patients during scanning). The network analysis will open the path to a new classification of patients. Indeed, we should start considering the complex

heterogeneity that characterizes the craniofacial complex. In this respect, anteroposterior skeletal patterns do not seem adequate to describe the craniofacial complex, even contemplating upper airway dimensions. Although cone beam computed tomography gave accessibility to three-dimensional data that are not possible to assess on lateral cephalograms, at the same time this increased the complexity in studying the craniofacial complex. For instance, the parameters necessary to understand the correlation between the upper airway and the craniofacial complex cannot be captured by a single approach.

Moreover, measuring dimensions can only describe one side of the complexity, and function might be incorporated to strengthen the possible relationships. Indeed, looking at our sample, by introducing the airway measurements, the network topology changed. Shortly, functional and geometrical features will need to be interconnected with airway physiology and/or pathophysiology, muscular and adipose tissue morphology (in this respect, the potentiality of MRI is evident) and genetic data.

The use of the network analysis showed promising results to describe the complex relationships between form and function. Further experimental research should aim to overcome the limitations of the present study, by using more extensive databases, both in terms of patients included and the amount and type of the parameters assessed. This will help clarifying whether the upper airway variations will respond to changes in the skeletal patterns, as the mathematical model seems to suggest.

5 | CONCLUSION

The application of the network analysis to analyse orthodontic and upper airway features can provide an intuitive visual representation of the orofacial system: it is possible to identify the most closely connected modules (features), highlighting the strength of interactions

existing among the modules. Results obtained from our sample support the development of alternative ways to classify subjects according to their craniofacial morphology and upper airway dimensions. The network analysis could potentially offer a powerful tool for implementing novel strategies for clinical practice and research in orthodontics.

CONFLICT OF INTEREST

The authors declare that they have no conflict of interest.

HUMAN AND ANIMAL RIGHTS AND INFORMED CONSENT

This article does not contain any experiments with animal subjects. The reported studies with human subjects performed by the authors complied with all applicable ethical standards (including the Helsinki Declaration and its amendments, institutional/national research committee standards and international/national/institutional guidelines).

DATA AVAILABILITY STATEMENT

The data sets presented and analysed in the current study have been previously analysed and published.²³ They are available from the corresponding author on reasonable request.

ORCID

Gabriele Di Carlo  <https://orcid.org/0000-0002-8039-7022>

Tommaso Gili  <https://orcid.org/0000-0001-9154-1758>

Guido Caldarelli  <https://orcid.org/0000-0001-9377-3616>

Antonella Polimeni  <https://orcid.org/0000-0002-2679-7607>

Paolo M. Cattaneo  <https://orcid.org/0000-0001-7604-3259>

REFERENCES

1. Niu X, Di Carlo G, Cornelis MA, Cattaneo PM. Three-dimensional analyses of short- and long-term effects of rapid maxillary expansion on nasal cavity and upper airway: a systematic review and meta-analysis. *Orthod Craniofac Res.* 2020;23(3):250-276.
2. Di Carlo G, Saccucci M, Ierardo G, et al. Rapid maxillary expansion and upper airway morphology: a systematic review on the role of cone beam computed tomography. *Biomed Res Int.* 2017;2017:e5460429.
3. van Vlijmen OJC, Kuijpers MAR, Bergé SJ, et al. Evidence supporting the use of cone-beam computed tomography in orthodontics. *J Am Dent Assoc.* 2012;143(3):241-252.
4. Di Carlo G, Gurani SF, Pinholt EM, Cattaneo PM. A new simple three-dimensional method to characterize upper airway in orthognathic surgery patient. *Dentomaxillofac Radiol.* 2017;46(8):e20170042.
5. Gurani SF, Cattaneo PM, Rafaelsen SR, Pedersen MR, Thorn JJ, Pinholt EM. The effect of altered head and tongue posture on upper airway volume based on a validated upper airway analysis-An MRI pilot study. *Orthod Craniofac Res.* 2020;23(1):102-109.
6. Zhang J, Chen G, Li W, Xu T, Gao X. Upper airway changes after orthodontic extraction treatment in adults: a preliminary study using cone beam computed tomography. *PLoS One.* 2015;10(11):e0143233.
7. Isidor S, Di Carlo G, Cornelis MA, Isidor F, Cattaneo PM. Three-dimensional evaluation of changes in upper airway volume in growing skeletal Class II patients following mandibular advancement treatment with functional orthopedic appliances. *Angle Orthod.* 2018;88(5):552-559.
8. Kapila SD, Nervina JM. CBCT in orthodontics: assessment of treatment outcomes and indications for its use. *Dentomaxillofac Radiol.* 2015;44(1):e20140282.
9. Joy A, Park J, Chambers DW, Oh H. Airway and cephalometric changes in adult orthodontic patients after premolar extractions. *Angle Orthod.* 2020;90(1):39-46.
10. Havron AG, Aronovich S, Shelgikar AV, Kim HL, Conley RS. 3D airway changes using CBCT in patients following mandibular setback surgery ± maxillary advancement. *Orthod Craniofac Res.* 2019;22(Suppl 1):30-35.
11. Grauer D, Cevidanes LSH, Styner MA, Ackerman JL, Proffit WR. Pharyngeal airway volume and shape from cone-beam computed tomography: relationship to facial morphology. *Am J Orthod Dentofacial Orthop.* 2009;136(6):805-814.
12. Claudino LV, Mattos CT, de Ruellas ACO, Sant' Anna EF. Pharyngeal airway characterization in adolescents related to facial skeletal pattern: a preliminary study. *Am J Orthod Dentofacial Orthop.* 2013;143(6):799-809.
13. Kim Y-J, Hong J-S, Hwang Y-I, Park Y-H. Three-dimensional analysis of pharyngeal airway in preadolescent children with different anteroposterior skeletal patterns. *Am J Orthod Dentofacial Orthop.* 2010;137(3):306.e1-11; discussion 306-7.
14. Hong J-S, Oh K-M, Kim B-R, Kim Y-J, Park Y-H. Three-dimensional analysis of pharyngeal airway volume in adults with anterior position of the mandible. *Am J Orthod Dentofacial Orthop.* 2011;140(4):e161-e169.
15. Oh K-M, Hong J-S, Kim Y-J, Cevidanes LSH, Park Y-H. Three-dimensional analysis of pharyngeal airway form in children with anteroposterior facial patterns. *Angle Orthod.* 2011;81(6):1075-1082.
16. Brito FC, Brunetto DP, Nojima MCG. Three-dimensional study of the upper airway in different skeletal Class II malocclusion patterns. *Angle Orthod.* 2019;89(1):93-101.
17. Alves PVM, Zhao L, O'Gara M, Patel PK, Bolognese AM. Three-dimensional cephalometric study of upper airway space in skeletal class II and III healthy patients. *J Craniofac Surg.* 2008;19(6):1497-1507.
18. Alves M Jr, Franzotti ES, Baratieri C, Nunes LKF, Nojima LI, Ruellas ACO. Evaluation of pharyngeal airway space amongst different skeletal patterns. *Int J Oral Maxillofac Surg.* 2012;41(7):814-819.
19. Linder-Aronson S. Respiratory function in relation to facial morphology and the dentition. *Br J Orthod.* 1979;6(2):59-71.
20. Ribbens KA, McNamara JA, Moyers RE, University of Michigan. *Naso-Respiratory Function and Craniofacial Growth: This Volume Includes the Proceedings of a Sponsored Symposium, Honoring Professor Robert E Moyers Held February 23 and 24, 1979, in Ann Arbor, Michigan.* Ann Arbor, Michigan: Center for Human Growth and Development, University of Michigan; 1979.
21. Warren D, Spalding P. Dentofacial morphology and breathing: a century of controversy. In: Melsen BE, ed. *Current Controversies in Orthodontics.* Chicago, IL: Quintessence Publishing; 45-76.
22. El H, Palomo JM. Airway volume for different dentofacial skeletal patterns. *Am J Orthod Dentofacial Orthop.* 2011;139(6):e511-21.
23. Di Carlo G, Polimeni A, Melsen B, Cattaneo PM. The relationship between upper airways and craniofacial morphology studied in 3D. A CBCT study. *Orthod Craniofac Res.* 2015;18(1):1-11.
24. Brasil DM, Kurita LM, Groppo FC, Haiter-Neto F. Relationship of craniofacial morphology in 3-dimensional analysis of the pharynx. *Am J Orthod Dentofacial Orthop.* 2016;149(5):683-691.e1.
25. Dalmau E, Zamora N, Tarazona B, Gandia JL, Paredes V. A comparative study of the pharyngeal airway space, measured with cone beam computed tomography, between patients with different craniofacial morphologies. *J Craniofac Surg.* 2015;43(8):1438-1446.



26. Blondel VD, Guillaume J-L, Lambiotte R, Lefebvre E. Fast unfolding of communities in large networks. *J Stat Mech*. 2008;2008(10):P10008.
27. Auconi P, Caldarelli G, Scala A, Ierardo G, Polimeni A. A network approach to orthodontic diagnosis. *Orthod Craniofac Res*. 2011;14(4):189-197.
28. Barabási A-L, Gulbahce N, Loscalzo J. Network medicine: a network-based approach to human disease. *Nat Rev Genet*. 2011;12(1):56-68.
29. Caldarelli G. *Scale-Free Networks*. Oxford, UK: Oxford University Press; 2013.
30. Auconi P, Scazzocchio M, Cozza P, McNamara JA Jr, Franchi L. Prediction of Class III treatment outcomes through orthodontic data mining. *Eur J Orthod*. 2015;37(3):257-267.
31. Sen A, Srivastava MS. *Regression Analysis*. Berlin, Germany: Springer; 2011.
32. Nicolini C, Forcellini G, Minati L, Bifone A. Scale-resolved analysis of brain functional connectivity networks with spectral entropy. *NeuroImage*. 2020;211:e116603.
33. Kuncheva LI, Hadjitodorov ST. Using diversity in cluster ensembles. In: 2004 IEEE International Conference on Systems, Man and Cybernetics (IEEE Cat. No.04CH37583). IEEE; 2005. <https://doi.org/10.1109/icsmc.2004.1399790>
34. Alexander-Bloch A, Lambiotte R, Roberts B, Giedd J, Gogtay N, Bullmore E. The discovery of population differences in network community structure: new methods and applications to brain functional networks in schizophrenia. *NeuroImage*. 2012;59(4):3889-3900.

How to cite this article: Di Carlo G, Gili T, Caldarelli G, Polimeni A, Cattaneo PM. A community detection analysis of malocclusion classes from orthodontics and upper airway data. *Orthod Craniofac Res*. 2021;00:1-9. <https://doi.org/10.1111/ocr.12490>